ELSEVIER

Biochimica et Biophysica Acta 1463 (2000) 197–208

BIOCHIMICA ET BIOPHYSICA ACTA
BBA

www.elsevier.com/locate/bba

Mechanism of hepatocellular uptake of albumin-bound bilirubin[1]

Stephen D. Zucker [a,*], Wolfram Goessling [b]

[a] *Division of Digestive Diseases, University of Cincinnati Medical Center, 231 Bethesda Avenue (ML 0595), Cincinnati, OH 45267-0595, USA*

[b] *Department of Medicine, Brigham and Women's Hospital, Boston, MA, USA*

Received 6 July 1999; received in revised form 30 September 1999; accepted 30 September 1999

Abstract

We previously demonstrated that unconjugated bilirubin spontaneously diffuses through phospholipid bilayers at a rate which exceeds albumin dissociation, suggesting that solvation from albumin represents the rate-limiting step in hepatic bilirubin clearance. To further examine this hypothesis, we studied the uptake of bovine serum albumin (BSA)-bound bilirubin by cultured hepatoblastoma (HepG2) cells. Uptake of bilirubin was saturable, with a K_m and V_{max} of 4.2 ± 0.5 μM ($\pm$S.E.M.) and 469 ± 41 pmol min^{-1} mg^{-1} at 25°C. Substantial bilirubin uptake also was observed at 4°C ($K_m = 7.0 \pm 0.8$ μM, $V_{max} = 282 \pm 26$ pmol min^{-1} mg^{-1}), supporting a diffusional transport mechanism. Consistent with reported solvation rates, the cellular uptake of bilirubin bound to human serum albumin was more rapid than for BSA-bound bilirubin, indicative of dissociation-limited uptake. Counterintuitively, an inverse correlation between pH and the rate of bilirubin flip-flop was observed, due to pH effects on the rate of dissociation of bilirubin from albumin and from the membrane bilayer. The identification of an inflection point at pH 8.1 is indicative of a pK_a value for bilirubin in this range. Taken together, our data suggest that hepatocellular uptake of bilirubin is dissociation-limited and occurs principally by a mechanism involving spontaneous transmembrane diffusion.

Keywords: Bilirubin; Uptake; pH; Diffusion; HepG2; Albumin

1. Introduction

Bilirubin IXα, the hydrophobic product of heme catabolism, is efficiently metabolized by the liver and secreted into bile as the water-soluble diglucuronide. The clearance of bilirubin by the liver is saturable and occurs against a concentration gradient [1–3], findings which support protein-mediated bilirubin transport across the basolateral (sinusoidal) membrane of the hepatocyte. Several putative bilirubin transporters have been identified and isolated [4–6] although none has yet been cloned or shown to specifically transport unconjugated bilirubin (UCB). Alternatively, it has been postulated that hepatocellular

Abbreviations: UCB, unconjugated bilirubin; HSA, human serum albumin; BSA, bovine serum albumin; cbBSA, Cascade blue-labeled BSA; PL, phospholipid; PBS, phosphate-buffered saline; dansyl-PE, *N*-(5-dimethylaminonaphthalene-1-sulfonyl) dipalmitoyl-L-α-phosphatidylethanolamine; BSP, bromosulfophthalein; BBBP, BSP/bilirubin binding protein

* Corresponding author. Fax: +1-513-558-1744; E-mail: zuckersd@email.uc.edu

[1] Preliminary reports of this work have been published in abstract form (W. Goessling, S.D. Zucker, Hepatology 26 (1997) 385A).

0005-2736/00/$ – see front matter
PII: S0005-2736(99)00196-0

bilirubin uptake occurs by spontaneous diffusion through the plasma membrane [7–10]. In support of this hypothesis, we have recently demonstrated that UCB diffuses rapidly through model and isolated native hepatocyte membrane vesicles via a mechanism involving flip-flop of the diacid species [11].

Based on an extension of the Bass-Pond diffusion model [12], Weisiger has proposed that hepatic uptake of certain ligands may be limited by dissociation from plasma binding proteins [13]. Our finding that the rate of bilirubin transmembrane diffusion exceeds the off-rate from serum albumin [14] led to the proposition that solvation from serum albumin represents the rate-limiting step in the clearance of UCB by the liver [11]. Indirect experimental evidence supporting dissociation-limited bilirubin transport is derived from studies demonstrating that uptake of bovine serum albumin (BSA)-bound bilirubin by the isolated, perfused rat liver is significantly slower than uptake of bilirubin solubilized in Fluosol-43 (in the absence of binding proteins) or bilirubin bound to ligandin [2], from which bilirubin dissociation is more rapid as compared with BSA [14,15]. Additionally, analbuminemic Nagase rats exhibit an enhanced rate of bilirubin clearance when compared with control animals possessing normal serum albumin levels [16].

While there have been a host of studies characterizing the transport and clearance of UCB in intact animals [1,17,18], in the perfused liver [2,3,18,19], and in isolated plasma membrane vesicles [11,20] there is a surprising paucity of information regarding bilirubin uptake at the cellular level. Iga et al. [21] found the uptake of UCB by cultured rat hepatocytes to be non-saturable and concluded that bilirubin transport occurs by transmembrane diffusion. However, these studies were performed in the *absence* of a protein carrier, and utilized bilirubin concentrations far in excess of the aqueous solubility. While other investigators have demonstrated uptake of UCB by cultured hepatocytes [4] and HepG2 cells [6] in the presence of albumin, kinetic analyses were not performed. In the present studies, we conduct cellular uptake analyses and utilize stopped-flow fluorescence techniques in order to determine bilirubin uptake kinetics and further characterize the mechanism(s) underlying the hepatocellular transport of UCB.

2. Materials and methods

2.1. Materials

Nigericin and essentially fatty acid-free bovine and human serum albumin were purchased from Sigma Chemical Company (St. Louis, MO). Bilirubin IXα was obtained from Porphyrin Products (Logan, UT), with purity ($>99.5\%$) assessed by absorbance in chloroform [10]. Grade 1 egg lecithin (phosphatidylcholine) was purchased from Lipid Products (Surrey, UK). Cascade blue-conjugated bovine serum albumin (cbBSA) and anti-Cascade blue antibodies were obtained from Molecular Probes (Eugene, OR). *N*-(5-Dimethylaminonaphthalene-1-sulfonyl) dipalmitoyl-L-α-phosphatidylethanolamine (dansyl-PE) was purchased from Avanti Polar Lipids (Birmingham, AL), and δ-[3,5-^{3}H]aminolevulinic acid from NEN Life Sciences (Boston, MA).

2.2. In vivo synthesis of radiolabeled bilirubin

[^{3}H]Bilirubin IXα was prepared by intravenous infusion of the metabolic precursor, δ-[3,5-^{3}H]aminolevulinic acid (250 μCi), into anesthetized male Sprague-Dawley rats (Charles River Breeding Laboratories, Wilmington, MA). Bile was collected for 6 h and bilirubin isolated by hydrolysis of glucuronides, precipitation with lead acetate, and extraction in chloroform [22,23]. Prepared in this manner, bilirubin specific activity ranged from 0.05 to 0.10 μCi $nmol^{-1}$, with purity assessed at over 98% by absorbance in chloroform solution. All steps were carried out in the dark to minimize bilirubin photodegradation.

2.3. Measurement of bilirubin uptake by HepG2 cells

Human hepatoblastoma (HepG2) cells were grown in Dulbecco's modified Eagle's medium supplemented with 10% fetal bovine serum, 1% non-essential amino acids, and 1% L-glutamine under 5% CO_2 to contain 2×10^6 cells per 35 mm dish ($\sim$70% confluent). Prior to uptake experiments, monolayers were washed repeatedly with phosphate-buffered saline (PBS) to remove residual albumin. The cells were then incubated at either 25°C or 4°C in PBS containing [^{3}H]bilirubin ($1–2\times10^5$ dpm) bound either to

bovine or human serum albumin. At various time intervals, the medium was rapidly removed and the cells washed twice with ice-cold PBS, followed by an additional wash with ice-cold PBS containing 5% BSA in order to completely displace surface-associated bilirubin. Further washes (with or without albumin) had no additional effect on cell associated radioactivity. Cells were dispersed with 0.1 M NaOH and counted in 20 ml of ScintiVerse II (Sigma Chemical Company). The quantity of bilirubin taken up by the cells was never more than 3% of the total added ($1–6\times10^3$ dpm per data point), ensuring that no significant depletion of bilirubin from the medium occurred over the time course of the experiments. Replicate plates were harvested for protein determination, using the assay method of Lowry et al. [24].

2.4. Affinity of human and bovine serum albumin for bilirubin

The relative affinity of human (HSA) and bovine serum albumin (BSA) for UCB was determined from the equilibrium binding. Partitioning was quantified by recording the steady-state fluorescence of bilirubin (ex: 467 nm, em: 525 nm) in the presence of varying molar ratios of the proteins, and fitting the data to the equation:

$$\frac{I_{HSA}-I_{BSA}}{I_{obs}-I_{BSA}} = 1+\left(\frac{K_a^{BSA}}{K_a^{HSA}}\right)\left(\frac{[BSA]}{[HSA]}\right) \quad (1)$$

where I_{HSA} and I_{BSA} represent the fluorescence intensity of bilirubin in the presence of HSA or BSA alone, I_{obs} reflects bilirubin fluorescence intensity at a defined molar ratio of BSA:HSA, K_a the association constant, and [BSA] and [HSA] the concentrations of bovine and human serum albumin, respectively. As the fluorescence intensity of bilirubin is dependent on the albumin species to which it is bound, the slope of a plot of $(I_{HSA}-I_{BSA})/(I_{obs}-I_{BSA})$ versus the molar ratio of BSA:HSA provides a direct measure of the relative affinity for bilirubin (K_a^{BSA}/K_a^{HSA}). The total albumin concentration ([HSA]+[BSA]) was maintained constant in order to control for inner filter effects resulting from intrinsic protein absorbance.

2.5. Isolation of white erythrocyte ghosts

Erythrocyte plasma membranes (ghosts) were isolated from 30 ml of human blood obtained from healthy volunteers, using a modification [25] of the method of Steck et al. [26]. The phlebotomy protocol and consent procedure were approved by the Brigham and Women's Hospital Human Research Committee (Protocol #96-07907). White (hemoglobin-deplete) erythrocyte ghosts were prepared in order to avoid potential competition between bilirubin and hemoglobin for binding to albumin [27]. No detectable hemoglobin was present in the preparation, as measured by the assay method of Riggs [28].

2.6. Preparation of small unilamellar phospholipid vesicles

Small unilamellar vesicles were prepared by probe sonication, as previously described [10]. A chloroform solution of phosphatidylcholine was evaporated to dryness under argon atmosphere, solubilized in ether, and re-evaporated to form a uniform film. The dried lipids were suspended in 0.1 M potassium phosphate solution and sonicated until clear. The vesicle suspension was centrifuged in order to sediment probe titanium particles and large vesicle contaminants, and the phospholipid concentration quantified by the assay method of Bartlett [29]. Fluorescent-labeled vesicles were prepared by incorporating dansyl-PE (0.5 mol%) at the time of sonication [10].

2.7. Stopped-flow analysis of bilirubin transmembrane diffusion

The rate of bilirubin transmembrane diffusion was determined from the time-dependent fluorescence changes associated with bilirubin equilibration between a suspension of small unilamellar phosphatidylcholine vesicles and cbBSA, as previously described [11]. UCB was incorporated into phospholipid vesicles by first dissolving bilirubin in alkaline (pH 12.0) potassium phosphate [10] and subsequently adding the solubilized bilirubin to small unilamellar phosphatidylcholine vesicles suspended in 0.1 M potassium phosphate buffered at pH 7.4 (unless otherwise indicated). The addition of a small

aliquot (≤1% v:v) of the bilirubin stock solution to the vesicle suspension caused no detectable alteration in the pH of the medium. An Aminco-Bowman II fluorescence spectrophotometer equipped with an SLM-Aminco MilliFlow stopped-flow reactor facilitated the rapid mixing of the bilirubin-containing vesicles with an equal volume of cbBSA solubilized in 0.1 M potassium phosphate. Bilirubin quenches cbBSA fluorescence (excitation: 380 nm, emission: 430 nm) in a concentration-dependent manner, such that the time-dependent diminution in Cascade blue fluorescence intensity reflects the combined process of bilirubin flip-flop from the internal to the external hemileaflet of the bilayer and subsequent dissociation and transfer from the external surface of the donor vesicles to cbBSA.

In order to specifically examine the process of bilirubin transmembrane flip-flop, data points were obtained every 200 ms [11] and the time course for bilirubin equilibration was analyzed by fitting the fluorescence curves to the function: $F(t) = \Sigma A_i \exp(-k_i t) + C$, where t is time, k_i the ith-order rate constant, A_i the amplitude, and C a constant term. Quality of fit was assessed by regression analysis, and an F-test applied to determine if the inclusion of an additional term provided a statistically significant improvement in curve fit [10]. As previously shown [11], the measured rate of equilibration (R) is dependent on the molar ratio of phospholipid:cbBSA:

$$R = \frac{\frac{K_a^{BSA}}{K_a^{PL}} + \frac{[PL]}{[BSA]}}{\frac{K_a^{BSA}}{K_a^{PL}}\left(\frac{1}{k_{ff}}\right) + \frac{[PL]}{[BSA]}\left(\frac{1}{k_{off}^{BSA}}\right)} \quad (2)$$

where K_a represents the affinity constant, k_{off} the dissociation rate constant, k_{ff} the flip-flop rate constant, and [BSA] and [PL] the concentrations of cbBSA and vesicle phospholipid, respectively. From Eq. 2 it is apparent that a plot of R versus [PL]/[BSA] intersects the y-axis at the flip-flop rate constant (k_{ff}), and asymptotically approaches the bilirubin dissociation rate constant from cbBSA (k_{off}^{BSA}) at high molar ratios of phospholipid:cbBSA.

The rate of solvation of UCB from phospholipid vesicles was determined from the fluorescence recordings of bilirubin equilibration between a suspension of 0.5 mol% dansyl-PE-labeled small unilamellar phosphatidylcholine donor vesicles and unlabeled acceptor vesicles, as previously described [10]. The binding of bilirubin to dansyl-labeled vesicles causes a reduction in fluorescence intensity due to resonance energy transfer between bilirubin and the dansyl moiety. The reemergence of dansyl fluorescence (excitation: 340 nm, emission: 525 nm) that occurs following the rapid mixing of the two vesicle populations reflects bilirubin transfer from the donor to the acceptor membranes. Due to the rapid rate of bilirubin solvation from phospholipid vesicles at pH 7.4 [10], analysis of bilirubin-membrane dissociation was performed with an Applied Photophysics (Leatherhead, UK) fluorescence spectrophotometer equipped with an SPF-17 stopped-flow device (mixing time: 0.7 ms).

3. Results

We have previously shown that the off-rate for UCB from human serum albumin is approximately five times slower than spontaneous transmembrane diffusion [11,14], suggesting that solvation from albumin represents the rate-limiting step in the hepatocellular clearance of bilirubin. To test this hypothesis, we examined the uptake of UCB by human hepatoblastoma (HepG2) cells, as this cell line has previously been shown to take up both bromosulfophthalein (BSP), a commonly used bilirubin surrogate, and bilirubin diglucuronide [6]. Human and bovine serum albumins were utilized as the bilirubin donor in these studies because of high-affinity binding and a nearly 10-fold difference in bilirubin dissociation rate [14].

3.1. Bilirubin uptake by HepG2 cells

Uptake studies were performed by incubating HepG2 monolayers in the presence of HSA- or BSA-bound [^{3}H]bilirubin IXα. At various time intervals, the medium was aspirated and the cells were washed, harvested, and counted. Bilirubin uptake at 25°C was rapid (Fig. 1), with a first-order rate constant of 0.27 ± 0.15 s^{-1} (±S.E.M.) for HSA-bound and 0.11 ± 0.01 s^{-1} for BSA-bound bilirubin. The measured uptake rate is unlikely to reflect cellular conjugation of bilirubin, which occurs over a more

protracted time course [30]. The 2.5-fold faster uptake of human versus bovine serum albumin-bound bilirubin cannot be explained by higher concentrations of free bilirubin in the presence of HSA, since this protein has a *greater* affinity for bilirubin than does BSA (Fig. 2). Indeed, when BSA serves as the carrier protein, total cellular uptake of bilirubin exceeds that observed with HSA (Fig. 1). The finding that the rate of cellular uptake is determined by the carrier protein to which bilirubin is bound is consistent with the concept of dissociation-limited transport [13].

Further evidence that bilirubin uptake is dissociation-limited is derived from the observation that the rate constant obtained for the uptake of BSA-bound bilirubin by HepG2 cells correlates closely with the previously reported off-rate for UCB from bovine serum albumin [14]. In contrast, the measured uptake rate for HSA-bound bilirubin is approximately threefold slower than predicted from the dissociation rate constant [14]. We believe that this discrepancy reflects the limitations of the experimental system utilized in our uptake studies, in that the earliest time point at which data can reliably be obtained is 8 s. As the half-time for bilirubin dissociation from BSA is ~7 s [14], the elapsed time interval before the first data point is acquired represents a single half-time. However, in the case of bilirubin solvation from HSA ($t_{1/2}$ = 750 ms), over 10 half-times elapse before the first data point is obtained. As a result of these technical limitations (which also hampered the determination of uptake at 37°C), we believe that the measured 25°C rate constant underestimates the actual rate of bilirubin uptake from HSA.

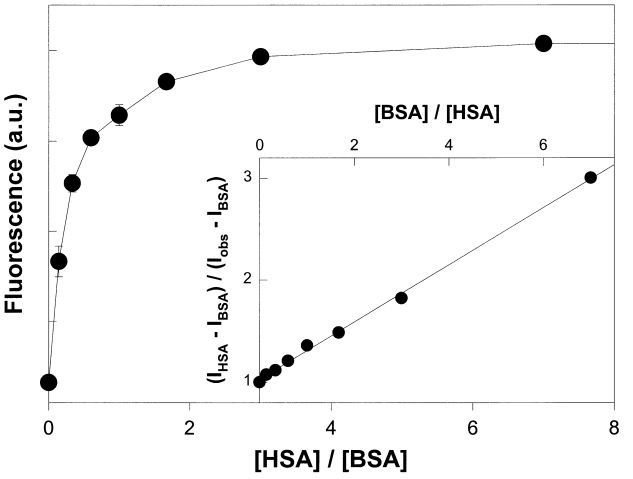

Fig. 2. Binding distribution of bilirubin between human and bovine serum albumin. The equilibrium distribution of UCB (2 μM) between human (HSA) and bovine (BSA) serum albumin was determined by measuring bilirubin steady-state fluorescence in the presence of varying molar ratios of HSA:BSA, maintaining the total albumin concentration constant at 16 μM. Each point, expressed in arbitrary fluorescence units (a.u.), represents the mean ± S.D. of three separate experiments performed at 25°C. In the inset, the fluorescence intensity ratio is plotted against the molar ratio of BSA:HSA. The relative affinity of the albumin species for bilirubin ($K_a^{BSA}/K_a^{HSA} = 0.29 \pm 0.005$; ± S.E.M.) is calculated from the slope ($r^2 = 0.997$) of the plot.

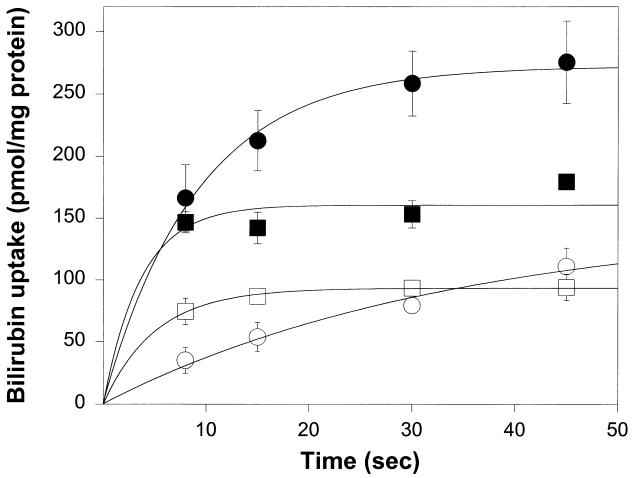

Fig. 1. Uptake of UCB by HepG2 cells. Cultured monolayers of HepG2 cells were incubated in the presence of [^{3}H]bilirubin IXα (8 μM) bound to human serum albumin (squares) or bovine serum albumin (circles) at a 1:1 molar ratio. Bilirubin uptake was calculated from the radioactivity present in the cell lysate following exhaustive washing. Data points reflect the mean (± S.D.) of three experiments performed at 25°C (filled symbols) or 4°C (open symbols) and are fit to single exponential functions (solid lines).

Substantial cellular transport of bilirubin also was detectable at 4°C (Fig. 1), with total uptake representing approximately 65% of that occurring at 25°C. The rate constants for the uptake of HSA-bound (0.20 ± 0.01 s^{-1}) and BSA-bound (0.026 ± 0.011 s^{-1}) bilirubin at 4°C correlate closely with bilirubin off-rates from the respective albumin species at this temperature [14]. This nearly eight-fold difference in uptake rate further supports that bilirubin transport is limited by dissociation from the albumin carrier. Indeed, the free energy of activation (18.8 kcal mol^{-1}) calculated [10] from the temperature dependence of the cellular uptake rate for BSA-bound bilirubin is

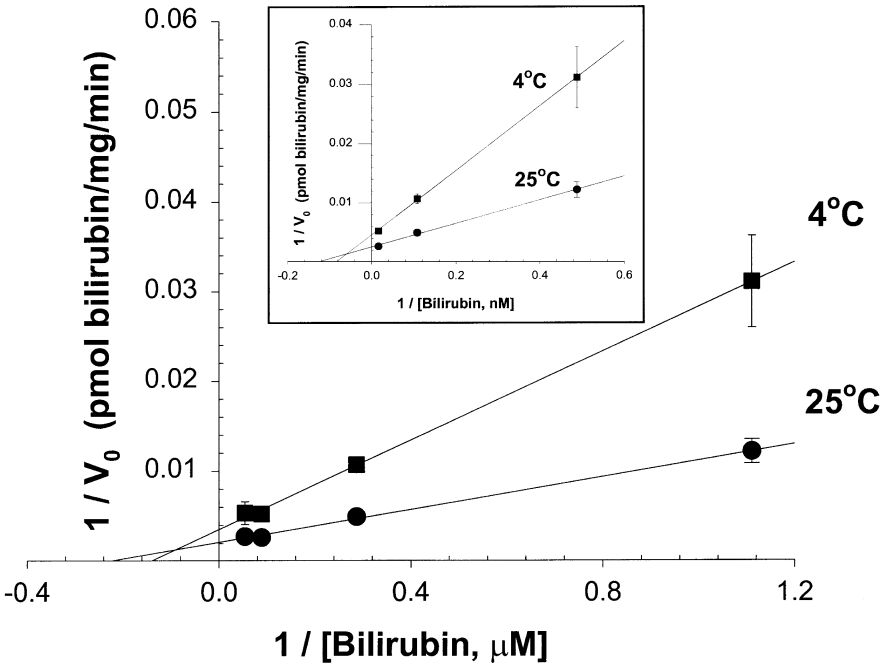

Fig. 3. Lineweaver-Burk plot of bilirubin uptake. The initial uptake velocity of BSA-bound [^{3}H]bilirubin IXα by HepG2 monolayers was measured over a range of bilirubin concentrations (0.9–18.5 μM), with the BSA concentration maintained at 18.5 μM. Data points reflect the mean ± S.D. of three separate experiments performed at 25°C (circles) and 4°C (squares). Based on linear regression analyses (solid lines) of these double reciprocal plots, the K_m and V_{max} for albumin-bound bilirubin uptake are 4.2 ± 0.5 μM and 469 ± 41 pmol min^{-1} mg^{-1} (± S.E.M.) at 25°C (r^2 = 0.998), and 7.0 ± 0.8 μM and 282 ± 26 pmol min^{-1} mg^{-1} at 4°C (r^2 = 0.999). The inset displays a reciprocal plot of the initial uptake rate versus the *free* bilirubin concentration, from which the K_m and V_{max} are calculated to be 7.9 ± 1.2 nM and 396 ± 44 pmol min^{-1} mg^{-1} at 25°C (r^2 = 0.998), and 11.9 ± 0.8 nM and 219 ± 12 pmol min^{-1} mg^{-1} at 4°C (r^2 = 0.999), respectively.

identical to that for bilirubin dissociation from BSA [14]. Additionally, the demonstration of significant bilirubin uptake at 4°C is consistent with a non-protein-mediated (diffusional) transport mechanism.

We subsequently examined the uptake of UCB by HepG2 cells over a range of bilirubin concentrations. In these studies, BSA was utilized as the bilirubin carrier as the slower uptake rate facilitated the determination of kinetic parameters. The initial uptake velocity (V_0) was obtained from the linear uptake of albumin-bound bilirubin over the first 15 s. From a double reciprocal plot of the data (Fig. 3), the K_m was calculated to be 4.2 ± 0.5 μM (± S.E.M.) at 25°C, consistent with physiologic serum bilirubin concentrations. Moreover, the V_{max} of 469 ± 41 pmol min^{-1} mg^{-1} is similar to hepatocellular uptake rates reported for other organic anions [6,31]. In order to determine the kinetic parameters for the uptake of unbound bilirubin, we calculated the free bilirubin concentration in these experiments. Using a consensus value for the BSA affinity constant of 2.5×10^7 M^{-1} [32,33], the concentration of free bilirubin was less than the reported aqueous solubility of 65 nM [34] at all but the highest total bilirubin concentration utilized (18.5 μM). When data points obtained at this bilirubin concentration are excluded, a double reciprocal plot of the initial uptake velocity versus the free bilirubin concentration (Fig. 3, inset) produces a K_m and V_{max} at 25°C of 7.9 ± 1.2 nM and 396 ± 44 pmol min^{-1} mg^{-1}, respectively. These results are highly concordant with the kinetic parameters obtained by investigators examining the uptake of UCB by rat basolateral plasma membrane vesicles [20].

While the finding that the quantity of bilirubin taken up at 4°C is less than the amount taken up at 25°C supports a potential role for specific plasma membrane transporters (which are inhibited at low temperatures) in the cellular uptake of bilirubin, the relatively modest reduction in V_{max} at 4°C and the

lack of a significant effect of temperature on K_m is atypical for protein-mediated transport [6]. Alternatively, our data can be explained by a relative decrease in the intracellular binding (or increase in the albumin binding) of bilirubin at 4°C, with the change in V_{max} reflecting the effect of temperature on the dissociation of bilirubin from BSA. Regardless, our results suggest that transmembrane diffusion accounts for well over one-half of the UCB taken up by HepG2 cells.

3.2. Bilirubin transport across erythrocyte plasma membranes

It has been argued that the rapid transport of bilirubin by hepatocytes, in the absence of demonstrable uptake by erythrocytes, supports the existence of specific bilirubin transporters in liver cells [35,36]. In an attempt to corroborate this assertion, we examined the transmembrane diffusion of UCB across

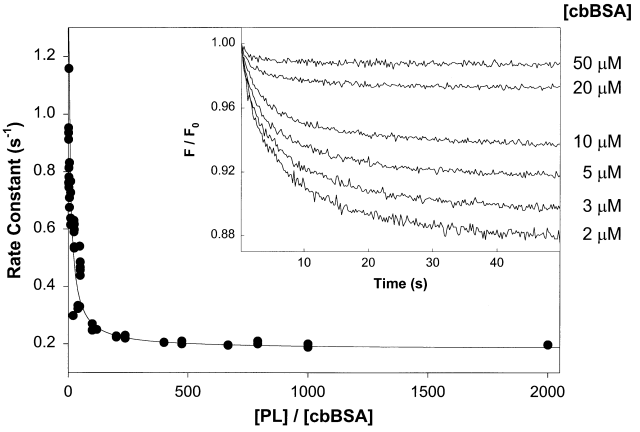

Fig. 4. Influence of the phospholipid:albumin molar ratio on the rate of bilirubin equilibration. The rate of equilibration of UCB (2 μM) between small unilamellar phosphatidylcholine vesicles and cbBSA was measured at 25°C over a range of phospholipid (PL) and albumin concentrations. The first-order rate constant is plotted against the molar ratio of phospholipid: albumin, with each point reflecting the mean of five stopped-flow injections. The curve (solid line) is generated from best-fit parameters for Eq. 2 ($P < 0.0005$): $k_{ff} = 1.5 \pm 0.1$ s^{-1}, $k_{off}^{BSA} = 0.17 \pm 0.03$ s^{-1}, $K_a^{BSA}/K_a^V = 64 \pm 23$ (± S.E.M.). The inset displays fluorescence recordings of bilirubin equilibration between phosphatidylcholine vesicles (1 mM phospholipid) and increasing concentrations of cbBSA (2–50 μM) obtained at 200 ms intervals. Each curve reflects the average of six stopped-flow injections and is expressed as the ratio of the fluorescence intensity versus the initial fluorescence at time 0.

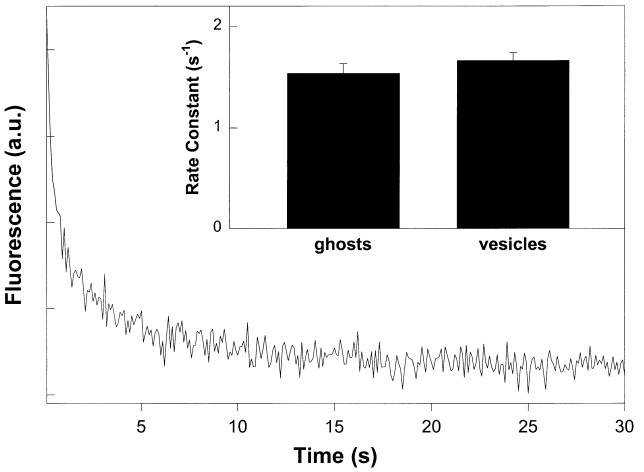

Fig. 5. Bilirubin transmembrane diffusion in erythrocyte ghosts. The rate of bilirubin diffusion across erythrocyte plasma membranes was determined by examining the equilibration of UCB (2 μM) between white (hemoglobin-deplete) erythrocyte ghosts (100 μM phospholipid) and free cbBSA (10 μM). A representative fluorescence tracing is presented, which reflects the average of five stopped-flow injections performed at 25°C. In the inset, the first-order rate constant for bilirubin flip-flop was found to be similar to that measured in small unilamellar phosphatidylcholine vesicles at equivalent phospholipid and cbBSA concentrations. Each bar represents the mean ± S.D. of three sets of experiments.

model phospholipid vesicles and isolated white (hemoglobin-deplete) erythrocyte ghosts. The equilibration of bilirubin between small unilamellar phosphatidylcholine donor vesicles and cbBSA was measured over a range of donor:acceptor concentrations, and the first-order rate constants plotted against the phospholipid:cbBSA molar ratio (Fig. 4). At low ratios of phospholipid:BSA, the equilibration rate (R) approaches the flip-flop rate constant, which is calculated to be 1.5 ± 0.1 s^{-1} (± S.E.M.) based on the best fit of the data to Eq. 2. This value for k_{ff} is lower than originally obtained using donor vesicles labeled with fluorescent phospholipids [11], a discrepancy which most likely reflects limitations in the present experimental system resulting from the diminished amplitude of the fluorescence signal at high cbBSA concentrations (Fig. 4, inset). At high phospholipid:BSA ratios, R asymptotically approaches 0.17 ± 0.03 s^{-1}, which correlates closely with values previously determined for k_{off}^{BSA} [11,14]. Employing a similar experimental approach, we examined bilirubin flip-flop in isolated erythrocyte ghosts (Fig. 5). We found that UCB is able to readily

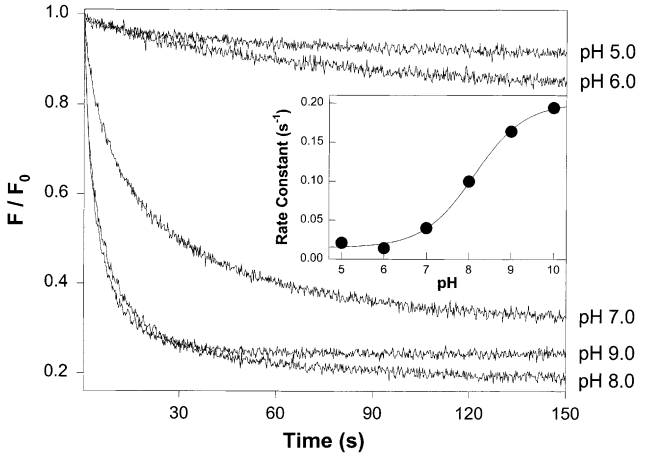

Fig. 6. Effect of pH on bilirubin equilibration. The effect of hydrogen ion concentration on the rate of UCB (2 μM) equilibration between small unilamellar phosphatidylcholine vesicles (1 mM phospholipid) and cbBSA (20 μM) was determined over a pH range of 5–10. Each curve represents the average of 10 stopped-flow injections performed at 25°C. In the inset, the rate constant for bilirubin transmembrane flip-flop is plotted versus pH, and fitted to a sigmoidal function (solid line). An inflection point is identified at pH 8.1.

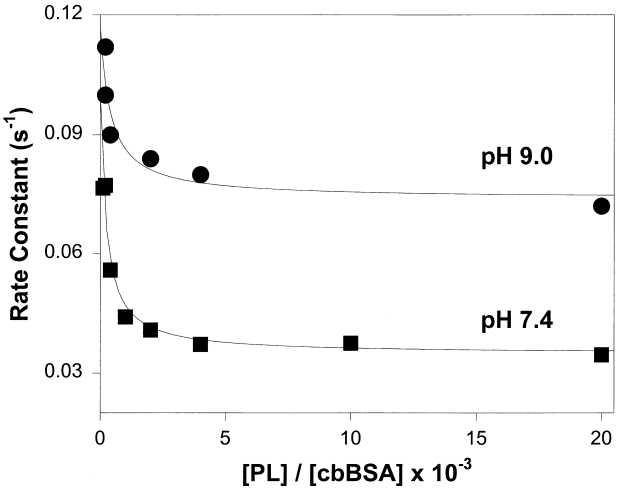

Fig. 7. Influence of pH on the kinetics of bilirubin equilibration. The equilibration of UCB (2 μM) between small unilamellar phosphatidylcholine vesicles (1 mM phospholipid) and cbBSA (0–10 μM) was measured at both pH 7.4 and pH 9.0, and rate constants plotted as a function of the ratio of phospholipid (PL) to cbBSA. Each point reflects the average of six stopped-flow injections, with the solid lines generated by fitting the data to Eq. 2.

diffuse through erythrocyte plasma membranes at a rate which is comparable to unilamellar phosphatidylcholine vesicles (Fig. 5, inset), indicating that bilirubin flip-flop is not unique to hepatocyte membranes.

3.3. Effect of pH on the kinetics of bilirubin flip-flop

We have previously demonstrated that bilirubin diffuses across phospholipid bilayers as the uncharged diacid [11]. Based on this mechanism, it is anticipated that bilirubin transmembrane flip-flop will be facilitated at low pH. We examined the effect of pH on bilirubin flip-flop kinetics by studying the equilibration of bilirubin between small unilamellar phosphatidylcholine vesicles and cbBSA over a pH range of 5–10 (Fig. 6). Surprisingly, the rate of bilirubin equilibration was found to *increase* in a sigmoidal fashion with increasing pH (Fig. 6, inset). To elucidate the mechanism whereby the hydrogen ion concentration of the medium influences the flip-flop rate, we examined the effect of pH on bilirubin equilibration between small unilamellar phosphatidylcholine vesicles and cbBSA over a range of cbBSA concentrations (Fig. 7). We found that the equilibration rate constants at pH 7.4 and 9.0 converge at the

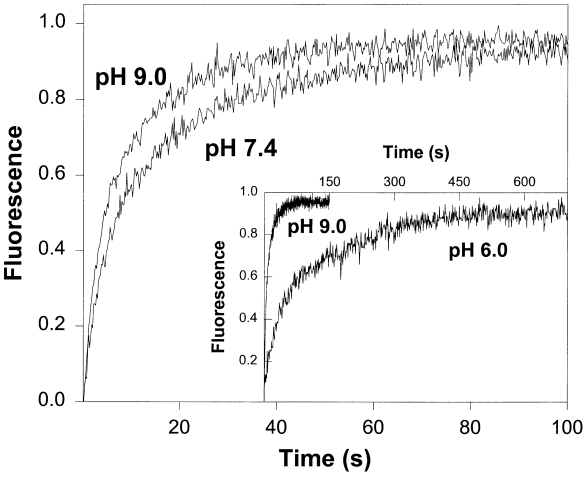

Fig. 8. Bilirubin dissociation from cbBSA: effect of pH. The rate of dissociation of UCB (1 μM) from cbBSA (1 μM) was measured using stopped-flow techniques. The reemergence of Cascade blue fluorescence reflects bilirubin transfer from cbBSA to a large molar excess of acceptor phosphatidylcholine vesicles (1 mM phospholipid). Each curve represents the average of five stopped-flow injections and is normalized to a scale of 0–1. Bilirubin dissociation from cbBSA is faster at pH 9.0 as compared with pH 7.4, with first-order rate constants of 0.132 ± 0.003 s^{-1} and 0.060 ± 0.001 s^{-1} ($\pm$S.E.M.), respectively. As shown in the inset, the dissociation rate constant at pH 6.0 (0.0076 ± 0.0001 s^{-1}) is over an order of magnitude slower than at pH 9.0.

y-intercept, suggesting that pH has a relatively modest effect on k_{ff}. In contrast, the value for k_{off}^{BSA} is nearly two times greater at pH 9.0 as compared with pH 7.4, indicating that the rate of bilirubin solvation from cbBSA decreases with increasing hydrogen ion concentration. This hypothesis was verified by directly examining the effect of pH on bilirubin dissociation from cbBSA (Fig. 8). Based on these findings, it appears that the effect of pH on the bilirubin equilibration rate is due, at least in part, to enhanced dissociation of bilirubin from cbBSA at low hydrogen ion concentrations.

Bilirubin IXα and other open-chain tetrapyrrole monomers exhibit a propensity to self-associate (aggregate) in aqueous solution [37]. At alkaline pH, aggregation is limited to the formation of reversible and thermodynamically stable dimeric complexes; however, at pH values below 8.3, self-association of bilirubin is characterized by the irreversible formation of insoluble, metastable colloids [38]. In order to determine whether the decline in the equilibration rate with decreasing pH might be attributable to bilirubin aggregation, we examined the effect of a pH jump on bilirubin equilibration between phosphatidylcholine vesicles and cbBSA. A suspension of small unilamellar vesicles were prepared at pH 6.0, loaded with bilirubin, and rapidly injected into a solution of cbBSA also buffered at pH 6.0 (Fig. 9A). As previously observed (Fig. 6), a slow decline in Cascade blue fluorescence is observed. Abruptly increasing the external pH to 9.0 with potassium hydroxide produces a sharp diminution in fluorescence, which remains unaffected by the further addition of enough nigericin (a proton/potassium ionophore) to completely collapse the pH gradient across the vesicle bilayer [11]. Since self-association of bilirubin monomers is irreversible at pH 6.0, aggregation should manifest as loss of the flip-flop signal. The rapid restoration of an equilibration curve following an increase in the pH of the external medium suggests that the slow equilibration rate observed at high hydrogen ion concentrations is not the result of bilirubin aggregation.

To further examine whether the pH *internal* to the vesicle controls the rate of bilirubin equilibration, bilirubin-incorporated vesicles were prepared at pH 9.0, and the external pH adjusted to 6.0 by abrupt dilution in a buffered solution of cbBSA, producing an instantaneous transmembrane pH gradient. Results similar to those observed with vesicles prepared at pH 6.0 were obtained (Fig. 9B). The additional finding that the fluorescence intensity of free cbBSA is unaffected by pH (Fig. 9C) confirms that these

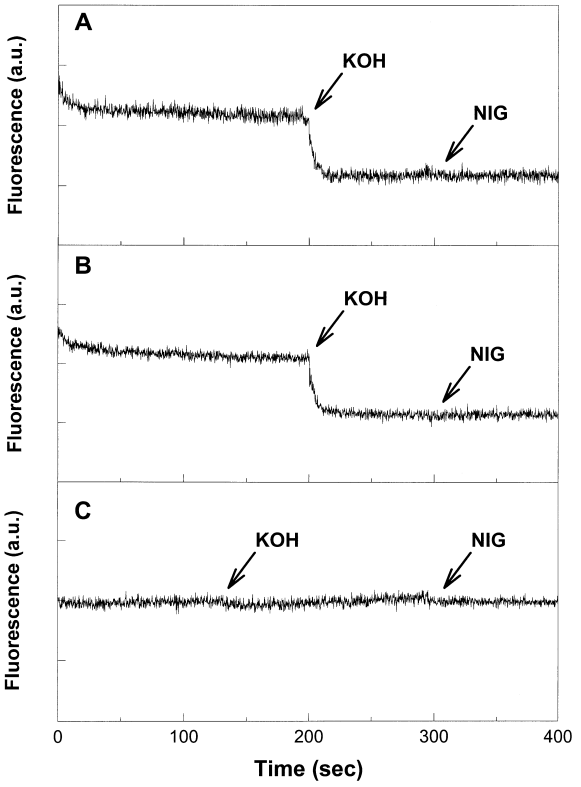

Fig. 9. Bilirubin equilibration between phospholipid vesicles and cbBSA: pH-jump analysis. (A) The effect of a rapid change in pH on UCB (2 μM) equilibration between small unilamellar phosphatidylcholine vesicles (1 mM phospholipid) and free cbBSA (20 μM) is shown. Vesicles were prepared in 0.1 M potassium phosphate (pH 6.0), and loaded with bilirubin. At time 0, 100 μl of the vesicle suspension was injected into 3 ml of a stirred solution of 20 μM cbBSA in 0.1 M potassium phosphate (pH 6.0). The pH of the medium subsequently was adjusted to pH 9.0 by the rapid injection of a small aliquot (5 μl) of potassium hydroxide (KOH). The addition of 3 μl (1 μg mg^{-1} phospholipid) nigericin (NIG) caused no additional change in fluorescence. (B) Similar results are obtained when bilirubin-containing vesicles are prepared at pH 9.0 and then added to a pH 6.0 buffered potassium phosphate solution containing cbBSA, thereby creating a transbilayer proton gradient. Addition of KOH to bring the external pH to 9.0 again induces a rapid decline in Cascade blue fluorescence, with no further effect of nigericin. (C) No change in fluorescence intensity occurs when a solution of cbBSA (20 μM), in the absence of vesicles or bilirubin, is subjected to a pH jump from 6.0 to 9.0 by the addition of KOH.

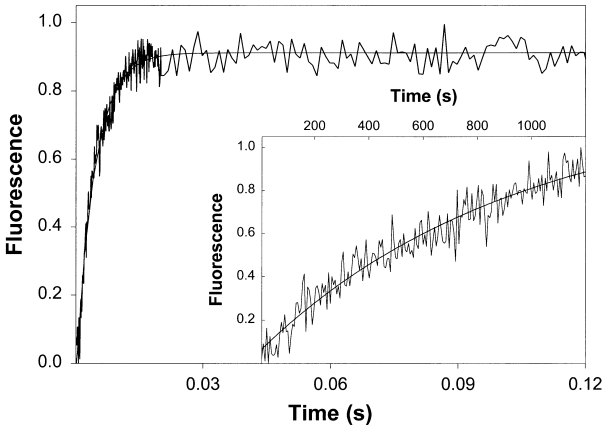

Fig. 10. Effect of pH on bilirubin solvation from phospholipid vesicles. The rate of bilirubin solvation from small unilamellar phosphatidylcholine vesicles was determined by monitoring the changes in fluorescence associated with the transfer of UCB (0.5 μM) from 0.5 mol% dansyl-PE-labeled vesicles (100 μM phospholipid) to unlabeled phosphatidylcholine vesicles (500 μM phospholipid). Vesicles were suspended in 0.1 M potassium phosphate (pH 7.4) and fluorescence intensity recorded over a time interval of 220 ms following the stopped-flow mixing of donor and acceptor membranes. The curve reflects the average of five injections conducted at 25°C and is best described by a single exponential function (solid line) with a first-order rate constant of 229 ± 5 s^{-1} (± S.E.M.). The inset displays the results of an identical experiment performed at pH 6.0, with the curve reflecting the average of three stopped-flow injections. The first-order rate constant of 0.0011 ± 0.0001 s^{-1} is calculated from a single exponential fit of the data (solid line). Curves are normalized to a scale of 0–1.

data reflect quenching of cbBSA by bilirubin rather than a nonspecific effect of pH on Cascade blue fluorescence. Based on these results, it appears that the pH of the medium external (rather than internal) to the vesicle is the key determinant of the bilirubin equilibration rate, suggesting that bilirubin solvation from the external hemileaflet of the vesicle bilayer is rate-limiting at low pH. Indeed, direct examination of the effect of hydrogen ion concentration on bilirubin solvation from phosphatidylcholine vesicles reveals that the dissociation rate constant declines by over five orders of magnitude as the pH is decreased from 7.4 to 6.0 (Fig. 10). Taken together, our findings indicate that the pH-dependent alterations in the rate of bilirubin equilibration between phospholipid vesicles and cbBSA represent the combined effect of diminished bilirubin dissociation from albumin *and* from the external surface of the donor vesicles at low pH, as opposed to a direct effect of pH on bilirubin transmembrane diffusion.

4. Discussion

The outlined experiments were designed to examine the influence of serum binding proteins on the kinetics of bilirubin uptake by HepG2 cell monolayers. Our prior observation that the rate of bilirubin transmembrane flip-flop [11] exceeds the off-rate from serum albumin [14] led to the proposition that solvation from albumin represents the rate-limiting step in the clearance of UCB by the liver. This hypothesis is supported by our demonstration that HepG2 cells take up HSA-bound bilirubin faster than BSA-bound bilirubin, and that the cellular uptake rate coincides with the rate of bilirubin dissociation from the proteins. Since the affinity of HSA for bilirubin exceeds that of BSA, the increased rate of bilirubin uptake from HSA cannot be due to higher free bilirubin concentrations. Taken together, these data suggest that hepatocellular uptake of albumin-bound bilirubin is determined by the rate of solvation from the protein, consistent with the concept of dissociation-limited uptake [13].

The fact that bilirubin uptake is limited by dissociation from its carrier underlies the paradoxical observation that the bilirubin equilibration rate decreases with increasing hydrogen ion concentration. We previously have shown that, at pH 7.4, the equilibration of UCB between membrane vesicles and albumin is limited by the rate of bilirubin transmembrane flip-flop [11]. In the present study, we demonstrate that the off-rate of bilirubin from albumin and from phospholipid bilayers decreases with the pH of the medium. Hence, as the pH is lowered, solvation of bilirubin from the membrane surface becomes rate-limiting and the equilibration rate declines, even though the actual flip-flop rate does not. Our data also provide insight into the acid-base properties of bilirubin IXα, the physiologic isomer of UCB. Based on [^{13}C]NMR analyses [39], the pK_a for mesobilirubin XIIIα, a structurally related bilirubin analog, was estimated to be in the range of 4.2–4.9, consistent with established pK_a values for a variety of other dicarboxylic acids. In contrast, the results of partitioning experiments suggest that the pK_a for the carboxyl moieties of bilirubin IXα are 8.1 and 8.4 [34], findings which are highly concordant with bilirubin aqueous solubility [37]. Proponents of these latter investigations have argued that the unusually high pK_a values for UCB result from the formation

of unique intramolecular hydrogen bonds [40]. Our pH studies indicate a transition point at pH 8.1, providing indirect support for the presence of a pK_a value in this range.

We have demonstrated that uptake of albumin-bound bilirubin by HepG2 cells is rapid and saturable, and that the K_m is compatible with normal physiologic bilirubin concentrations. Both the initial rate and the quantity of UCB taken up by HepG2 cells at 4°C are approximately two-thirds of that measured at 25°C. The fact that bilirubin uptake is saturable and temperature-dependent has been construed as evidence for the existence of a specific membrane transporter(s) [20]. Since two putative bilirubin transport proteins, BSP/bilirubin binding protein (BBBP) and bilitranslocase, are expressed by HepG2 cells [6,41], there exists the possibility that these proteins facilitate bilirubin uptake in this cell line. Indeed, this hypothesis fits nicely with data demonstrating that pretreatment of HepG2 monolayers or isolated hepatocyte cultures with antibodies to BBBP decreases the cellular uptake of UCB by 30–40% [4,6].

On the other hand, diffusional processes also have been shown to exhibit 'saturation' kinetics [42,43]. Furthermore, while it is reasonable to conclude that uptake at 4°C is diffusional in nature (since protein-mediated transport typically is negligible at this temperature), the converse assumption, that increased bilirubin uptake observed at higher temperatures reflects the additional activity of a transporter, is not necessarily valid. Indeed, our data suggest that simple diffusion cannot be distinguished from protein-mediated uptake using an experimental approach where albumin serves as the bilirubin donor. This is because the measured uptake rate reflects bilirubin dissociation from human (or bovine) serum albumin which, at 25°C, is over five-fold (50-fold) slower than transmembrane transport [11]. Hence, the increase in V_{max} observed at 25°C as compared with 4°C can be readily explained by the more rapid dissociation of bilirubin from albumin at higher temperatures [14]. This hypothesis is supported by the observation that the rate of cellular uptake for albumin-bound bilirubin corresponds closely with the bilirubin off-rate from albumin at both 4°C and 25°C. Moreover, the relatively modest decrease in K_m at higher temperatures is less than would be expected if transport was protein-mediated. The finding that substantial uptake of UCB occurs at 4°C, representing 60–70% of total uptake at 25°C, provides additional support for a non-specific diffusional uptake mechanism [7,11,21]. While our results do not exclude a contribution of specific membrane transporters, they do suggest that hepatocellular bilirubin uptake occurs principally by transmembrane diffusion; thereby providing an explanation for the diffuse yellow staining observed in a wide variety of tissues in patients with hyperbilirubinemia [44,45]. Indeed, despite reports to the contrary [35,36], our analyses indicate that red cell membranes are freely permeable to UCB, consistent with the original observations of Wennberg [7].

The proposition that a significant proportion of cellular bilirubin uptake occurs by passive diffusion is supported by the findings of a number of investigators. For example, nonspecific uptake, as defined by the absence of saturation [21], non-antibody inhibitable uptake [4], uptake by non-transfected control cells [46], or cellular uptake at 4°C [20], represents a sizeable proportion of total cellular bilirubin uptake in most in vitro transport studies. It has further been shown that UCB is able to rapidly diffuse through model phospholipid vesicles in the absence of transport proteins [9,11,47,48], and that phospholipid acyl saturation, lipid packing, and cholesterol concentration have little impact on bilirubin flip-flop kinetics [11]. Both free and BSA-bound UCB are taken up by HeLa cells [46], which do not express any of the putative bilirubin transport proteins. Moreover, at physiologic bilirubin concentrations, Gunn rat fibroblasts transduced to express UDP-glucuronosyltransferase activity are able to conjugate bilirubin at a rate equivalent to that of normal hepatocytes [30], implying efficient uptake of UCB. Finally, data regarding the biliary excretion of various bilirubin analogs by normal versus Gunn rats [49] provide additional in vivo support for a diffusional mechanism of bilirubin transport into the hepatocyte. In conjunction with the present studies, these observations provide ample support for the hypothesis that a substantial component of bilirubin uptake occurs via transmembrane diffusion. Precise delineation of the role that transport-proteins play in the uptake of UCB await the results of cloning and functional expression studies.

Acknowledgements

The authors gratefully acknowledge Dr. Alison Hoppin for her seminal contributions to this work. This study was supported by National Institutes of Health Research Grants DK-51679 (S.D.Z.), a Charles H. Hood Foundation Child Health Research Award (S.D.Z.), a Harvard Digestive Diseases Center Pilot/Feasibility Grant (S.D.Z.), and by a BASF Foundation Postdoctoral Research Award (W.G.).

References

[1] B.F. Scharschmidt, J.G. Waggoner, P.D. Berk, J. Clin. Invest. 56 (1975) 1280–1292.
[2] Y.R. Stollman, U. Gartner, L. Theilmann, N. Ohmi, A.W. Wolkoff, J. Clin. Invest. 72 (1983) 718–723.
[3] G. Paumgartner, J. Reichen, Clin. Sci. Mol. Med. 51 (1976) 169–176.
[4] W. Stremmel, P.D. Berk, J. Clin. Invest. 78 (1986) 822–826.
[5] G.A. Kullak-Ublick, B. Hagenbuch, B. Stieger, A.W. Wolkoff, P.J. Meier, Hepatology 20 (1994) 411–416.
[6] W. Stremmel, H.E. Diede, J. Hepatol. 10 (1990) 99–104.
[7] R.P. Wennberg, Pediatr. Res. 23 (1988) 443–447.
[8] R. Schmid, New Engl. J. Med. 287 (1972) 703–709.
[9] D. Hayward, D. Schiff, S. Fedunec, G. Chan, J.P. Davis, M.J. Poznansky, Biochim. Biophys. Acta 860 (1986) 149–153.
[10] S.D. Zucker, J. Storch, M.L. Zeidel, J.L. Gollan, Biochemistry 31 (1992) 3184–3192.
[11] S.D. Zucker, W. Goessling, A.G. Hoppin, J. Biol. Chem. 274 (1999) 10852–10862.
[12] R.A. Weisiger, S.M. Pond, L. Bass, Am. J. Physiol. 257 (1989) G904–G916.
[13] R.A. Weisiger, Proc. Natl. Acad. Sci. USA 82 (1985) 1563–1567.
[14] S.D. Zucker, W. Goessling, J.L. Gollan, J. Biol. Chem. 270 (1995) 1074–1081.
[15] S.D. Zucker, W. Goessling, B.J. Ransil, J.L. Gollan, J. Clin. Invest. 96 (1995) 1927–1935.
[16] M. Inoue, E. Hirata, Y. Morino, S. Nagase, J.R. Chowdhury, N.R. Chowdhury, I.M. Arias, J. Biochem. 97 (1985) 737–743.
[17] P.D. Berk, R.B. Howe, J.R. Bloomer, N.I. Berlin, J. Clin. Invest. 48 (1969) 2176–2190.
[18] J. Gollan, L. Hammaker, V. Licko, R. Schmid, J. Clin. Invest. 67 (1981) 1003–1015.
[19] U. Gartner, R.J. Stockert, W.G. Levine, A.W. Wolkoff, Gastroenterology 83 (1982) 1163–1169.
[20] L. Pascolo, S. del Vecchio, R.K. Koehler, E.J. Bayon, C.C. Webster, P. Mukerjee, J.D. Ostrow, C. Tiribelli, Biochem. J. 316 (1996) 999–1004.
[21] T. Iga, D.L. Eaton, C.D. Klaassen, Am. J. Physiol. 236 (1979) C9–C14.
[22] J.D. Ostrow, L. Hammaker, R. Schmid, J. Clin. Invest. 40 (1961) 1442–1452.
[23] J.M. Crawford, B.J. Ransil, C.S. Potter, S.V. Westmoreland, J.L. Gollan, J. Clin. Invest. 79 (1987) 1172–1180.
[24] O.H. Lowry, N.J. Rosebrough, A.L. Farr, R.J. Randall, J. Biol. Chem. 193 (1951) 265–275.
[25] G. Fairbanks, T.L. Steck, D.F.H. Wallach, Biochemistry 10 (1971) 2604–2617.
[26] T.L. Steck, R.S. Weinstein, J.H. Straus, D.F. Wallach, Science 168 (1970) 255–257.
[27] Z. Hrkal, S. Klementova, Int. J. Biochem. 16 (1984) 799–804.
[28] A. Riggs, Methods Enzymol. 76 (1981) 5–29.
[29] G.R. Bartlett, J. Biol. Chem. 234 (1959) 466–468.
[30] J. Seppen, K. Tada, S. Hellwig, C.T.M. Bakker, V.R. Prasad, N. Roy-Chowdhury, J. Roy-Chowdhury, P.J. Bosma, R.P.J. Oude Elferink, Biochem. J. 314 (1996) 477–483.
[31] A.D. Min, T. Goeser, R. Liu, C.G. Campbell, P.M. Novikoff, A.W. Wolkoff, Hepatology 14 (1991) 1217–1223.
[32] R.F. Chen, in: A.A. Thaer, M. Sernetz (Eds.), Fluorescence Techniques in Cell Biology, Springer-Verlag, Berlin, 1973, pp. 273–282.
[33] T. Faerch, J. Jacobsen, Arch. Biochem. Biophys. 168 (1975) 351–357.
[34] J.S. Hahm, J.D. Ostrow, P. Mukerjee, L. Celic, J. Lipid Res. 33 (1992) 1123–1137.
[35] G.L. Sottocasa, S. Passamonti, L. Battiston, L. Pascolo, C. Tiribelli, J. Hepatol. 24 (1996) 36–41.
[36] G. Baldini, S. Passamonti, G.C. Lunazzi, C. Tiribelli, G.L. Sottocasa, Biochim. Biophys. Acta 856 (1996) 1–10.
[37] M.C. Carey, W. Spivak, in: J.D. Ostrow (Ed.), Bile Pigments and Jaundice: Molecular, Metabolic and Medical Aspects, Marcel Dekker, New York, 1986, pp. 81–132.
[38] M.C. Carey, A.P. Koretsky, Biochem. J. 179 (1979) 675–689.
[39] D.A. Lightner, D.L. Holmes, A.F. McDonagh, J. Biol. Chem. 271 (1996) 2397–2405.
[40] J.D. Ostrow, P. Mukerjee, C. Tiribelli, J. Lipid Res. 35 (1994) 1715–1737.
[41] P. Marchegiano, F. Carubbi, C. Tiribelli, S. Amarri, M. Stebel, G.C. Lunazzi, D. Levy, S. Bellentani, Biochem. Biophys. Res. Commun. 183 (1992) 1203–1208.
[42] B. Maisterrena, L.J. Blum, P.R. Coulet, Biochem. J. 242 (1987) 835–839.
[43] D. Zakim, Proc. Soc. Exp. Biol. Med. 212 (1996) 5–14.
[44] S.B. Turkel, Clin. Perinatol. 17 (1990) 381–396.
[45] R.G. Harper, E.I. Kahn, C.G. Sia, D. Horn, R. Villi, C.A. Hessel, Arch. Pathol. Lab. Med. 110 (1986) 614–617.
[46] N. Kanai, R. Lu, Y. Bao, A.W. Wolkoff, V.L. Schuster, Am. J. Physiol. 270 (1996) F319–F325.
[47] N. Noy, M. Leonard, D. Zakim, Biophys. Chem. 42 (1992) 177–188.
[48] S.D. Zucker, W. Goessling, M.L. Zeidel, J.L. Gollan, J. Biol. Chem. 269 (1994) 19262–19270.
[49] A.F. McDonagh, D.A. Lightner, Cell. Mol. Biol. 40 (1994) 965–974.